

Another look at the three-gluon vertex in the minimal Landau gauge

Guilherme T. R. Catumba,^{a,b} Orlando Oliveira^b and Paulo J. Silva^{b,*}

^a*IFIC - University of Valencia - Spain*

^b*CFisUC, Department of Physics, University of Coimbra, 3004-516 Coimbra, Portugal*

E-mail: gtelo@ific.uv.es, orlando@uc.pt, psilva@uc.pt

The lattice three-gluon vertex in the Landau gauge is revisited using a large physical volume $\sim (8\text{fm})^4$ and a large statistical ensemble. The improved calculation explores the symmetries of the hypercubic lattice to reduce the statistical uncertainties and addresses the evaluation of the lattice artefacts. Special attention is given to the low energy behaviour of the vertex and its relation to ghost dominance.

*The 38th International Symposium on Lattice Field Theory, LATTICE2021 26th-30th July, 2021
Zoom/Gather@Massachusetts Institute of Technology*

*Speaker

1. Introduction

The three-gluon vertex is one of the QCD fundamental Green's functions. This vertex allows the computation of the strong coupling constant and the measurement of a static potential between color charges. Herein we report on an upgrade of the lattice computation of this vertex performed by some of the authors in [1, 2].

The three-gluon correlation function $G_{\mu_1\mu_2\mu_3}^{a_1a_2a_3}(p_1, p_2, p_3)$ is given by

$$\langle A_{\mu_1}^{a_1}(p_1) A_{\mu_2}^{a_2}(p_2) A_{\mu_3}^{a_3}(p_3) \rangle = V \delta(p_1 + p_2 + p_3) G_{\mu_1\mu_2\mu_3}^{a_1a_2a_3}(p_1, p_2, p_3) \quad (1)$$

and can be written in terms of the gluon propagator $D_{\mu\nu}^{ab}(p^2)$ and the one-particle irreducible (1PI) vertex Γ using

$$G_{\mu_1\mu_2\mu_3}^{a_1a_2a_3}(p_1, p_2, p_3) = D_{\mu_1\nu_1}^{a_1b_1}(p_1) D_{\mu_2\nu_2}^{a_2b_2}(p_2) D_{\mu_3\nu_3}^{a_3b_3}(p_3) \Gamma_{\nu_1\nu_2\nu_3}^{b_1b_2b_3}(p_1, p_2, p_3). \quad (2)$$

Bose symmetry requires the 1PI vertex to be symmetric under permutations of any pair (p_i, a_i, μ_i) . Given that

$$\Gamma_{\mu_1\mu_2\mu_3}^{a_1a_2a_3}(p_1, p_2, p_3) = f_{a_1a_2a_3} \Gamma_{\mu_1\mu_2\mu_3}(p_1, p_2, p_3) \quad (3)$$

then the function $\Gamma_{\mu_1\mu_2\mu_3}(p_1, p_2, p_3)$ must be antisymmetric under the interchange of any pair (p_i, μ_i) .

A complete description of $\Gamma_{\mu_1\mu_2\mu_3}(p_1, p_2, p_3)$ in the continuum requires six Lorentz invariant form factors, two associated to the transverse component $\Gamma^{(t)}$ and the remaining associated to the longitudinal $\Gamma^{(l)}$ [3].

2. Asymmetric momentum configuration

In this work we consider the computation of the three-gluon vertex in the asymmetric momentum configuration $p_2 = 0$, as in [1, 4]. In this case, the correlation function can be written as

$$G_{\mu_1\mu_2\mu_3}(p, 0, -p) = V \frac{N_c(N_c^2 - 1)}{4} [D(p^2)]^2 D(0) \frac{\Gamma(p^2)}{3} p_{\mu_2} T_{\mu_1\mu_3}(p). \quad (4)$$

The contraction of the Lorentz μ_1 and μ_3 indices, together with the contraction with the momentum p_α , gives

$$G_{\mu\alpha\mu}(p, 0, -p) p_\alpha = V \frac{N_c(N_c^2 - 1)}{4} [D(p^2)]^2 D(0) \Gamma(p^2) p^2. \quad (5)$$

From this expression it is possible to extract the form factor $\Gamma(p^2)$. However, a lattice measurement of $\Gamma(p^2)$ requires the computation of the ratio

$$G_{\mu\alpha\mu}(p, 0, -p) p_\alpha / [D(p^2)]^2 D(0) \quad (6)$$

and the extraction of $\Gamma(p^2)$ from this ratio will originate large statistical fluctuations at high momenta, where $D(p^2)$ becomes quite small. In fact, assuming Gaussian error propagation, it is possible to show that the statistical error on $\Gamma(p^2)$ behaves as $\Delta\Gamma(p^2) \sim p^4$ in the UV regime [1].

3. Handling of noise, lattice artefacts

In order to try to deal with the large statistical fluctuations at high momenta, we considered a few strategies [5]:

- explore the ambiguity on the scale setting and perform a binning in the momentum — all data points in each bin are replaced by a weighted average of the data points;
- perform a $H(4)$ extrapolation of the lattice data [6, 7] — such procedure is based on the remnant $H(4)$ symmetry group associated with a hypercubic lattice. On the lattice, a scalar quantity F is a function of the $H(4)$ invariants

$$p^2 = p^{[2]} = \sum_{\mu} p_{\mu}^2, \quad p^{[4]} = \sum_{\mu} p_{\mu}^4, \quad p^{[6]} = \sum_{\mu} p_{\mu}^6, \quad p^{[8]} = \sum_{\mu} p_{\mu}^8,$$

i.e. $F_{Lat} = F(p^{[2]}, p^{[4]}, p^{[6]}, p^{[8]})$. The continuum limit will be given by $F(p^{[2]}, 0, 0, 0)$ up to corrections $\mathcal{O}(a^2)$. Having several data points for the same p^2 but different $p^{[4]}, p^{[6]}, p^{[8]}$, an extrapolation of F_{Lat} to the continuum limit can be done, assuming that it can be written as a power series of the $H(4)$ invariants. Note that, in this work, only a linear extrapolation in $p^{[4]}$ is considered.

4. Lattice setup

In this work we consider the 64^4 ensemble of 2000 configurations already studied in [1], together with a 80^4 ensemble of 1800 configurations, both generated with the Wilson gauge action at $\beta = 6.0$. The rotation to the Landau gauge has been performed using the Fourier accelerated Steepest Descent method [8] implemented with the help of Chroma [9] and PFFT [10] libraries. The gluon field is computed using the definition

$$ag_0 A_{\mu}(x + a\hat{e}_{\mu}) = \frac{U_{\mu}(x) - U^{\dagger}(x)}{2ig_0} - \frac{\text{Tr} [U_{\mu}(x) - U^{\dagger}(x)]}{6ig_0} \quad (7)$$

with the momentum space gluon field given by

$$A_{\mu}(\hat{p}) = \sum_x e^{-i\hat{p}(x+a\hat{e}_{\mu})} A_{\mu}(x + a\hat{e}_{\mu}), \quad \hat{p}_{\mu} = \frac{2\pi n_{\mu}}{aL_{\mu}}. \quad (8)$$

5. Results

In Figure 1 we compare the original and binned data for $\Gamma(p^2)$. The binning of the data suppresses the large statistical errors in the high momentum region and produces a well defined and smooth curve.

Next, in Figure 2 we compare the binned data for both lattices. The results of the two volumes agree within errors, suggesting that finite volume effects are small.

In Figure 3 we compare the $H(4)$ extrapolation of the 64^4 lattice data with the binning of the original data. We observe that the $H(4)$ extrapolation pushes the vertex to higher values in the high momentum regime. Nevertheless, in the infrared region, the extrapolated data is compatible with the original data, for both lattice volumes — see Figure 4.

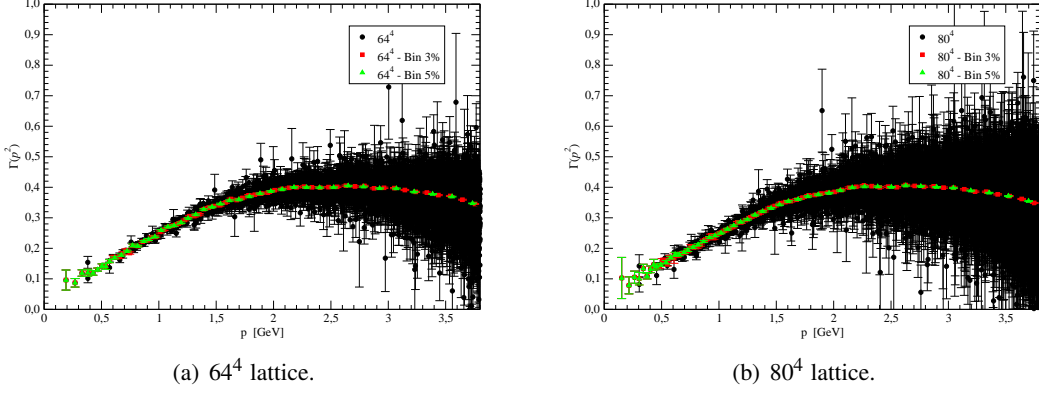


Figure 1: Original and binned data for $\Gamma(p^2)$.

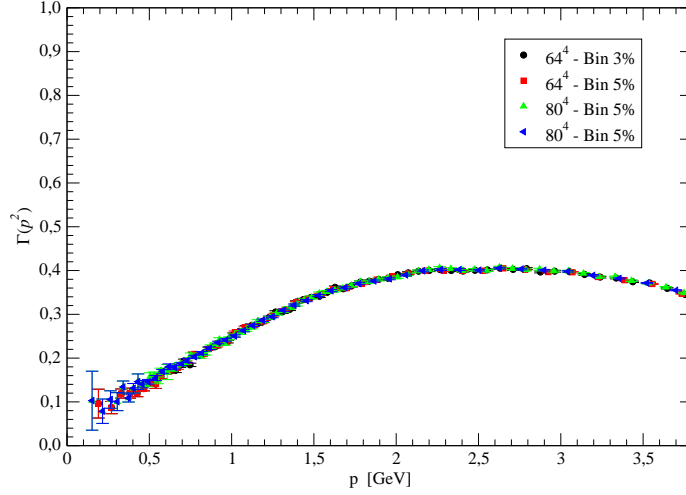


Figure 2: Comparison of binned data for $\Gamma(p^2)$.

6. Infrared behaviour of $\Gamma(p^2)$

No zero crossing of $\Gamma(p^2)$, an indication of ghost dominance in the infrared, is seen in the lattice data reported here. In order to check for a change of sign in $\Gamma(p^2)$, in this section we explore the infrared behaviour of the lattice $\Gamma(p^2)$, using the 80^4 data for momenta below 1 GeV, and fit the data to $\Gamma_1(p^2) = A + Z \ln(p^2)$ and $\Gamma_2(p^2) = A + Z \ln(p^2 + m^2)$. The first one is a typical ansatz considered in recent studies to study the zero crossing, see [5] for details, and the second one is a variant of the first one which includes an infrared logarithmic regularizing mass.

In Figure 5 we plot the best fits of the lattice data for both fitting functions, obtained through the minimization of $\chi^2/d.o.f.$. For $\Gamma_1(p^2)$, we got $\chi^2/d.o.f. = 1.23$ with $A = 0.2395(16)$ and $Z = 0.0646(21)$. Accordingly the zero crossing occurs at $p_o = 157\text{MeV}$. For $\Gamma_2(p^2)$, the parameters take the values $A = 0.208(24)$, $Z = 0.124(27)$ and $m = 0.61(15)\text{GeV}$, with a $\chi^2/d.o.f. = 0.95$.

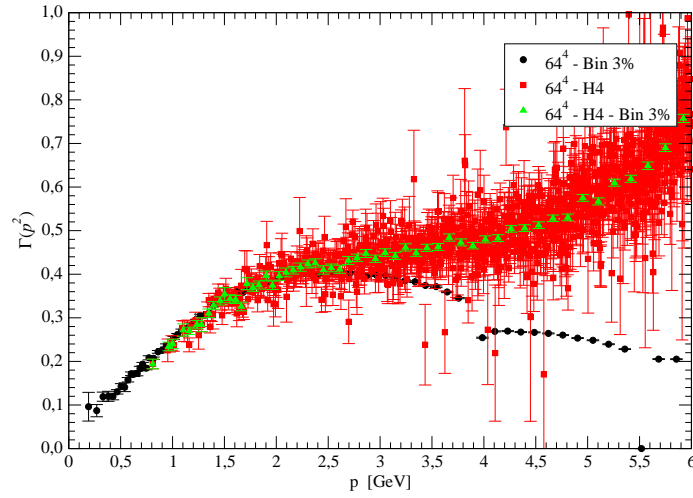


Figure 3: Results of the H(4) extrapolation of $\Gamma(p^2)$ on the 64^4 lattice volume.

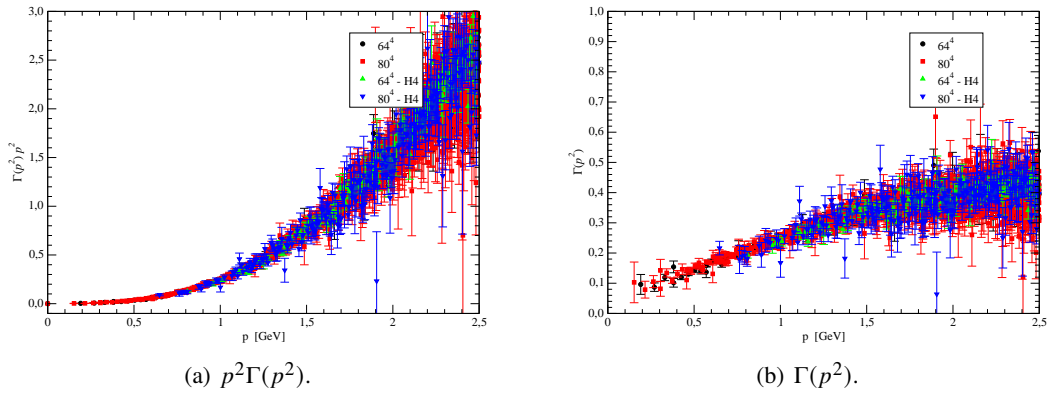


Figure 4: Original and H(4) data for both lattice volumes for low momenta.

As shown in the right plot of Figure 5, in this case there is no zero crossing.

7. Conclusions and outlook

In this paper we describe an improved calculation of the three gluon vertex on the lattice, for the asymmetric momentum configuration. We use two different lattice volumes $(6.5 \text{ fm})^4$ and $(8.2 \text{ fm})^4$, with a common lattice spacing of $a = 0.102 \text{ fm}$. We show that a H(4) extrapolation of the lattice data pushes the vertex to higher values in UV regime. We proceed with a functional study in the infrared region, considering some functional forms compatible with zero crossing and IR divergence.

Further momentum configurations will be explored in the near future.

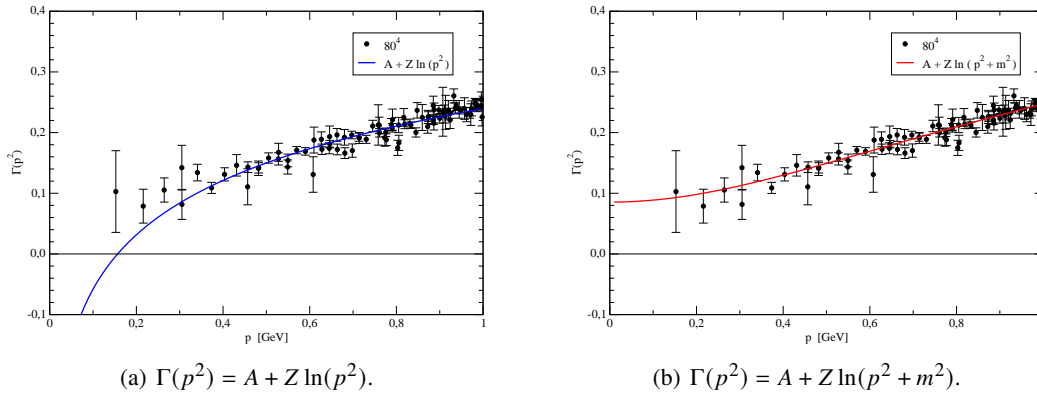


Figure 5: Infrared 80^4 lattice data for $\Gamma(p^2)$ together with some fitting functions.

Acknowledgments

This work was supported by national funds from FCT Fundação para a Ciência e a Tecnologia, I. P., within the Projects UIDB/04564/2020, UIDP/04564/2020, and CERN/FIS-COM/0029/2017. G. T. R. C. acknowledges financial support from FCT under Project UIDB/04564/2020, and also from the Generalitat Valenciana (genT program CIDEGENT/2019/040) and Ministerio de Ciencia e Innovacion PID2020-113644GB-I00. P. J. S. acknowledges financial support from FCT under Contract CEECIND/00488/2017. This work was granted access to the HPC resources of the PDC Center for High Performance Computing at the KTH Royal Institute of Technology, Sweden, made available within the Distributed European Computing Initiative by the PRACE-2IP, receiving funding from the European Communitys Seventh Framework Programme (FP7/2007-2013) under Grant agreement no. RI-283493. The use of Lindgren has been provided under DECI-9 project COIMBRALATT. We acknowledge that the results of this research have been achieved using the PRACE-3IP project (FP7 RI312763) resource Sisu based in Finland at CSC. The use of Sisu has been provided under DECI-12 project COIMBRALATT2. We acknowledge the Laboratory for Advanced Computing at the University of Coimbra [11] for providing access to the HPC resource Navigator. The authors acknowledge Minho Advanced Computing Center [12] for providing HPC resources that have contributed to the research results reported within this paper. This work was produced with the support of MACC and it was funded by FCT I.P. under the Advanced Computing Project CPCA/A2/6816/2020, platform Bob. This work was produced with the support of INCD [13] funded by FCT and FEDER under the project 01/SAICT/2016 n° 022153.

References

- [1] A. G. Duarte, O. Oliveira, P. J. Silva, Phys. Rev. **D94** (2016) 074502.
- [2] A. G. Duarte, O. Oliveira, P. J. Silva, [PoS\(LATTICE2016\)351](#).
- [3] J. S. Ball, T.-W. Chiu, Phys. Rev. **D22** (1980) 2550.

-
- [4] B. Allés, D. S. Henty, H. Panagopoulos, C. Parrinello, C. Pittori, D. G. Richards, Nucl. Phys. **B502** (1997) 325.
- [5] Guilherme Telo Rodrigues Catumba, Master Thesis, University of Coimbra, 2020, arXiv:2101.06074 [hep-lat].
- [6] D. Becirevic, Ph. Boucaud, J. P. Leroy, J. Micheli, O. Pène, J. Rodríguez-Quintero, C. Roiesnel, Phys. Rev. **D60** (1999) 094509.
- [7] F. de Soto and C. Roiesnel, JHEP **09** (2007) 007.
- [8] C. T. H. Davies, G. G. Batrouni, G. R. Katz, A. S. Kronfeld, G. P. Lepage, K. G. Wilson, P. Rossi, B. Svetitsky, Phys. Rev. **D37** (1998) 1581.
- [9] R. G. Edwards, B. Joo, Nucl. Phys. Proc. Suppl. **140** (2005) 832, arXiv:hep-lat/0409003.
- [10] M. Pippig, SIAM J. Sci. Comput. **35** (2013) C213.
- [11] <https://www.uc.pt/lca>
- [12] <https://macc.fccn.pt>
- [13] <https://www.incd.pt>